



**HAL**  
open science

## **Provenance study of oyster shells by LA-ICP-MS**

Vincent Mouchi, Camille Godbillot, Catherine Dupont, Marc-Antoine Vella, Vianney Forest, Alexey Ulianov, Franck Lartaud, Marc de Rafélis, Laurent Emmanuel, Eric P. Verrecchia

► **To cite this version:**

Vincent Mouchi, Camille Godbillot, Catherine Dupont, Marc-Antoine Vella, Vianney Forest, et al.. Provenance study of oyster shells by LA-ICP-MS. *Journal of Archaeological Science*, 2021, 132, pp.105418. 10.1016/j.jas.2021.105418 . hal-03284352

**HAL Id: hal-03284352**

**<https://hal.science/hal-03284352>**

Submitted on 8 Sep 2021

**HAL** is a multi-disciplinary open access archive for the deposit and dissemination of scientific research documents, whether they are published or not. The documents may come from teaching and research institutions in France or abroad, or from public or private research centers.

L'archive ouverte pluridisciplinaire **HAL**, est destinée au dépôt et à la diffusion de documents scientifiques de niveau recherche, publiés ou non, émanant des établissements d'enseignement et de recherche français ou étrangers, des laboratoires publics ou privés.

# Provenance study of oyster shells by LA-ICP-MS

Vincent Mouchi<sup>1\*</sup>, Camille Godbillot<sup>1</sup>, Catherine Dupont<sup>2</sup>, Marc-Antoine Vella<sup>3</sup>, Vianney Forest<sup>4</sup>, Alexey Ulianov<sup>5</sup>, Franck Lartaud<sup>6</sup>, Marc de Rafélis<sup>7</sup>, Laurent Emmanuel<sup>1</sup>, Eric P. Verrecchia<sup>8</sup>

<sup>1</sup>: Sorbonne Université, CNRS-INSU, Institut des Sciences de la Terre Paris, IStEP, F-75005 Paris, France

<sup>2</sup>: CNRS, CReAAH, UMR 6566, Université de Rennes, F-35042 Rennes, France

<sup>3</sup>: Sorbonne Université, CNRS, EPHE, UMR 7619 METIS, F-75005 Paris, France

<sup>4</sup>: INRAP-Midi-Méditerranée, UMR 5068, TRACES, F-31000 Toulouse, France

<sup>5</sup>: University of Lausanne, Institut des Sciences de la Terre, CH-1015, Lausanne, Switzerland

<sup>6</sup>: Sorbonne Université, CNRS, Laboratoire d'Ecogéochimie des Environnements Benthiques, LECOB, F-66650, Banyuls, France

<sup>7</sup>: Géosciences Environnement Toulouse, CNRS, IRD, Université Paul Sabatier Toulouse 3, 14 Avenue Edouard Belin, F-31400 Toulouse, France

<sup>8</sup>: University of Lausanne, Institut des Dynamiques de la Surface Terrestre, CH-1015, Lausanne, Switzerland

\*: Corresponding author: [vmouchi@gmail.com](mailto:vmouchi@gmail.com); Current address: Sorbonne Université, CNRS, UMR 7144, Station Biologique de Roscoff, Place Georges Teissier, F-29680, Roscoff, France

## ABSTRACT

Provenance determination of archaeological remains is a valuable tool for reconstruction of past exchange networks. Among these materials, oyster shells are ubiquitous in sites from all

24 prehistorical and historical periods. Thus, they seem to be as promising candidates for provenance  
25 identification as they include chemical elements from the environment in their shells, which implies  
26 that an elemental fingerprint of the region of origin can be recorded in the shell composition. In this  
27 study, we present elemental measurements from 15 groups of modern and archaeological shells from  
28 13 continental localities in mainland France and the island of Corsica (western Mediterranean Sea).  
29 Two of these localities had two oyster species (*Crassostrea gigas* and *Ostrea edulis*). Results indicate  
30 that (i) a species-specific elemental fingerprint exists and (ii) the Atlantic Ocean and Mediterranean  
31 Sea provenances can be identified for *O. edulis* shells. Moreover, if the shell originated from a locality  
32 only partially connected to the ocean (*e.g.* an estuary or lagoon), a fingerprint specific to the watershed  
33 can also be observed, even between groups originating from the same bay. Using these measurements  
34 as reference fingerprints, we characterize the Mediterranean origin of two groups of shells unearthed at  
35 Lyons (central France, 200 km away from the nearest shoreline), dated from the 1<sup>st</sup> c. CE.

36

## 37 1. INTRODUCTION

38 Reconstruction of exchange networks in archaeology is paramount to study large-scale  
39 medium- to long-term economics, as well as cultural and technological transfers, since routes were  
40 vectors of ideas and cultural exchanges. Numerous studies have attempted to reconstruct the  
41 provenance of marbles (Herz and Waelkens, 1988; Matthews, 1997; Mrozek-Wysocka, 2014),  
42 obsidian (Robin et al., 2016; Kuzmin et al., 2018), variscite (Querré et al., 2015), ceramics (Michelaki  
43 et al., 2013), and ore (Vogl et al., 2019). Yet, only a few studies have focused on shells and shell beads  
44 from chemical analyses (Shackleton and Renfrew, 1970; Eerkens et al., 2005).

45 In Mesolithic and Neolithic sites from the European Atlantic seaboard, food wastes composed  
46 of oyster shells are exclusively found on the coastline (Dupont, 2016) as the hunter-gatherer  
47 populations consumed the soft body and discarded the shell on site. More recent sites from Antiquity  
48 comprise oyster shells used for consumption in numerous localities, even distant from marine shores  
49 (Bardot-Cambot, 2014). Indeed, during this period, oysters were consumed by the elite as delicacies

50 away from the sea (Bardot-Cambot, 2014). Most of the time, the provenance of these archaeological  
51 shells remains unknown, unless these shells are associated with other taxa, (epi-)fauna, or substrate  
52 that presents some endemic characteristics possibly identified by specialists (Schneider and Lepetz,  
53 2007; Bardot-Cambot, 2013; Chaufourier et al., 2015; Somerville et al., 2017). However, these  
54 identifications require substantial knowledge in cladistics as well as in the geological settings of the  
55 shoreline at regional to country (even sometimes continental) scales, as it is known that high-level  
56 dignitaries in Rome were used to import oysters from countries as far as England (Andrews, 1948;  
57 André, 1981). In the more common case of non-endemic associated items, archaeologists rely on  
58 morphometry to identify groups of shells of different origins (Gruet and Prigent, 1986a, 1986b;  
59 Bardot-Cambot, 2014). Nonetheless, such characteristics are not specific to a locality but rather, to the  
60 type of substrate (Gruet and Prigent, 1986a; Campbell, 2010; Somerville et al., 2017); therefore, they  
61 are not relevant to the geographical identification of the specimen's origin beyond a single region.

62 Other techniques have been developed in order to identify the provenance of shell remains,  
63 such as geochemical analyses, not only for archaeology (Eerkens et al., 2005, 2010; Mouchi et al.,  
64 2020a), but also for quality control of modern cultured specimens prior to market distribution  
65 (Bennion et al., 2019; Morrison et al., 2019). In addition, geochemistry has been used to study  
66 connectivity of separated populations of mollusc species that colonize distant localities through larval  
67 dispersion (Becker et al., 2005; Carson, 2010; Fodrie et al., 2011; Sorte et al., 2013).

68 Molluscs build their shells in calcium carbonate by sampling chemical elements from their  
69 surrounding waters, and the shell's chemical composition reflects (at least partially) that of the  
70 environment (Urey et al., 1951). Most studies have used oxygen and carbon stable isotope ratios ( $\delta^{18}\text{O}$   
71 and  $\delta^{13}\text{C}$ , respectively) from shells as a provenance proxy (Eerkens et al., 2005, 2010; Bajnóczi et al.,  
72 2013; Milano et al., 2019; Apolinarska and Kurzawska, 2020), but the use of this approach appears to  
73 be restricted to differentiate between marine and brackish/estuarine environments. Indeed,  $\delta^{18}\text{O}$  and  
74  $\delta^{13}\text{C}$  are mainly representative of local biogeochemical conditions rather than the geographical  
75 location (temperature and salinity for  $\delta^{18}\text{O}$  and food source for  $\delta^{13}\text{C}$ ; Craig, 1965; Sharp, 2007;  
76 Lartaud et al., 2010a). Temporal homogeneity for the regional fingerprint cannot be insured as

77 seasonal temperatures have an impact on  $\delta^{18}\text{O}$ , leading to the overlap of amplitude values with remote  
78 areas exhibiting similar seasonal temperature contrasts (Mouchi et al., 2020b). Additionally, it was  
79 recently demonstrated that oysters do not mineralize their shell in equilibrium with seawater during  
80 their first year of growth, making unlikely the use of  $\delta^{18}\text{O}$  as a proxy for local physicochemical  
81 conditions during this life stage (Huyghe et al., 2020). Overall, elemental analyses tend to provide  
82 better results in provenance determination than carbon and oxygen isotopic compositions (Zhao and  
83 Zhang, 2016; Ricardo et al., 2017; Bennion et al., 2019; Morrison et al., 2019). Nevertheless, such  
84 studies have identified issues related to ‘vital effects’: the metabolism acts as a filter between the  
85 living environment and the shell, thus modifying the shell’s final composition. It has indeed been  
86 shown (Mouchi et al., 2020a) that concentrations in rare earth elements (REE) can be used to identify  
87 the region of provenance for the cupped oyster *Crassostrea gigas*. Still, these elements are not  
88 discriminant for the flat oyster, *Ostrea edulis*, which is the only oyster species found in European  
89 archaeological sites, as the cupped oyster *Crassostrea angulata* was imported to Portugal from Asia  
90 during the 17<sup>th</sup> century. Consequently, other chemical elements need to be investigated as provenance  
91 proxies for *O. edulis*.

92 In the present study, we use a new multi-elemental approach based on laser-ablation  
93 inductively-coupled plasma mass spectrometry (LA-ICP-MS) performed on 68 modern and  
94 archaeological oyster specimens (*C. gigas* and *O. edulis*) from 15 groups of different localities and  
95 ages. We aim at using this approach to identify potential discriminant elements for provenance studies  
96 applied to both oyster species found in Europe. This technique was selected as it is fast and commonly  
97 used in carbonate geochemistry studies (Durham et al., 2017).

98

## 99 2. MATERIALS AND METHODS

### 100 **2.1. Collection sites and specimens**

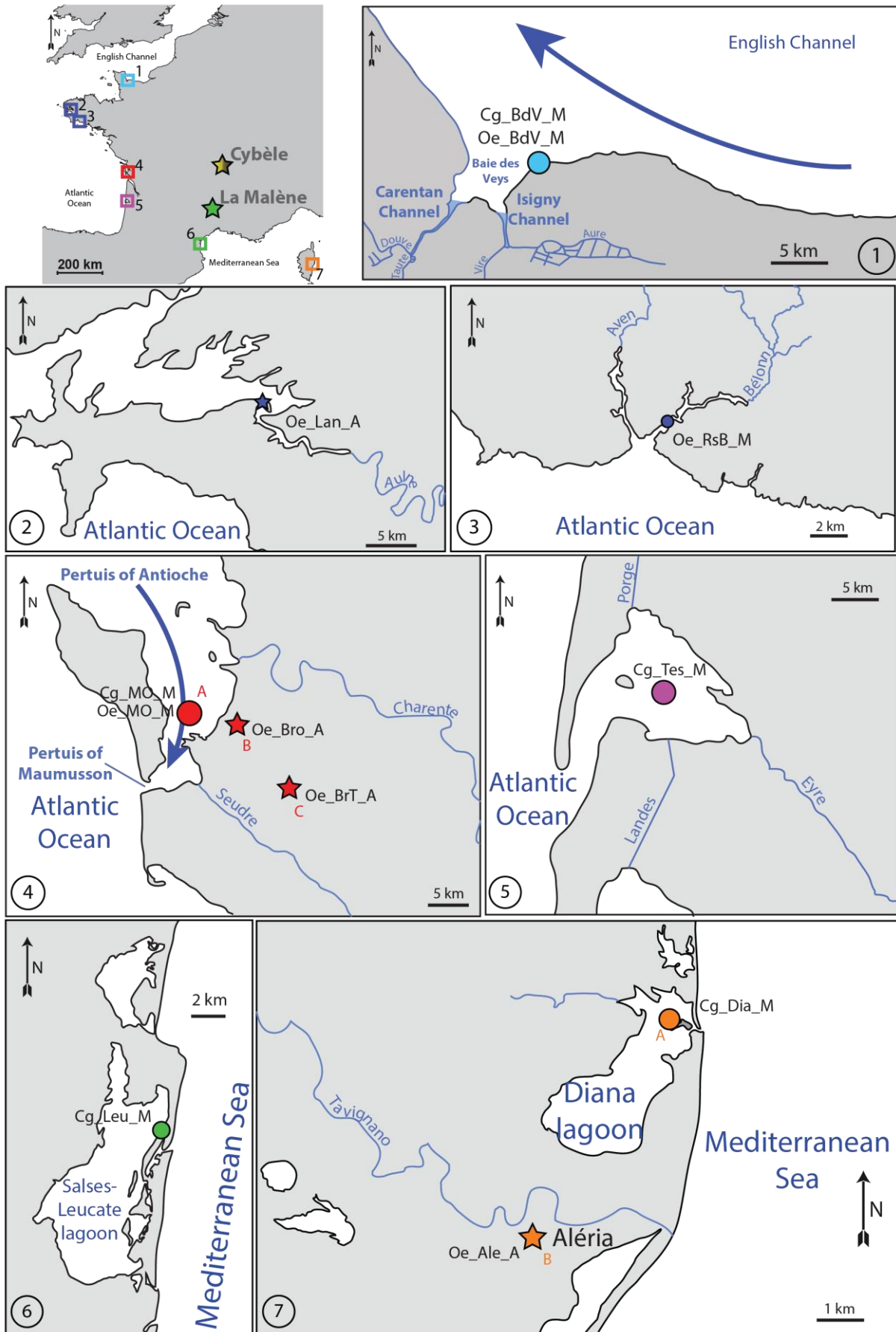
101 Samples were collected from multiple modern localities and archaeological sites in continental  
102 France and the island of Corsica (**Figure 1; Table 1**). As elemental composition of the rivers

103 (suggested to influence the composition of seawater and shells at the output) reflects the composition  
 104 of substrate weathered on land, a brief description of the geological formations of watersheds are  
 105 indicated with site descriptions in **Supplementary Information 1**. Specimens are divided into groups  
 106 of origin, according to their species ('Cg' and 'Oe' for *C. gigas* and *O. edulis*, respectively), their  
 107 locality (see **Table 1**), and their age ('M' for modern and 'A' for ancient specimens). Although the  
 108 species *Crassostrea gigas* has been recently renamed *Magallana gigas* (Salvi and Mariottini, 2016),  
 109 this genus change is debated by numerous experts (Bayne et al., 2017), so we will continue to use the  
 110 name *Crassostrea gigas* throughout the paper.

111 **Table 1:** Number of specimens and measurements per group of shells.

| Group    | Location                            | Coordinates            | ID on Figure 1 | Age                                       | Number of specimens | Number of measurements |
|----------|-------------------------------------|------------------------|----------------|---|---------------------|------------------------|
| Cg_BdV_M | Baie des Veys (Normandy)            | 49°23.11 N, 01°06.05 W | 1              | Modern                                    | 5                   | 38                     |
| Oe_BdV_M | Baie des Veys (Normandy)            | 49°23.11 N, 01°06.05 W | 1              | Modern                                    | 5                   | 38                     |
| Oe_Lan_A | Landévennec (Brittany)              | 48°17.42 N, 04°16.00 W | 2              | 8 <sup>th</sup> – 15 <sup>th</sup> c. CE  | 2                   | 16                     |
| Oe_RsB_M | Riec-sur-Bélon (Brittany)           | 47°48.55 N, 03°43.08 W | 3              | Modern                                    | 3                   | 20                     |
| Cg_MO_M  | Marennes-Oléron (Charente-Maritime) | 45°52.23 N, 01°10.60 W | 4A             | Modern                                    | 3                   | 23                     |
| Oe_MO_M  | Marennes-Oléron (Charente-Maritime) | 45°52.23 N, 01°10.60 W | 4A             | Modern                                    | 3                   | 16                     |
| Oe_Bro_A | Brouage (Charente-Maritime)         | 55°85.05 N, 01°07.44 W | 4B             | 16 <sup>th</sup> c. CE                    | 4                   | 24                     |
| Oe_BrT_A | Broue tower (Charente-Maritime)     | 45°47.67 N, 00°58.57 W | 4C             | 11 <sup>th</sup> – 14 <sup>th</sup> c. CE | 6                   | 40                     |
| Cg_Tes_M | Tès (Arcachon Basin)                | 44°40.01 N, 01°08.18 W | 5              | Modern                                    | 8                   | 70                     |
| Cg_Leu_M | Leucate (Aude)                      | 42°52.48 N, 03°01.50 E | 6              | Modern                                    | 5                   | 35                     |
| Cg_Dia_M | Diana lagoon (Corsica Island)       | 42°08.00 N, 09°32.17 E | 7A             | Modern                                    | 2                   | 13                     |
| Oe_Ale_A | Aléria (Corsica Island)             | 42°06.50 N, 09°30.72 E | 7B             | Antiquity                                 | 2                   | 14                     |
| Oe_X1_A  | Unknown                             | Unknown                | -              | 1 <sup>st</sup> c. CE                     | 6                   | 45                     |
| Oe_X2_A  | Unknown                             | Unknown                | -              | 1 <sup>st</sup> c. CE                     | 8                   | 41                     |
| Oe_Mal_A | Undefined (Mediterranean Sea)       | Unknown                | -              | 6 <sup>th</sup> c. CE                     | 6                   | 39                     |

112



114 **Figure 1:** Sample collection sites. Modern specimen groups are indicated by circles while archaeological specimen groups  
115 are presented as stars. Colour coding corresponds to that used in the t-SNE analysis on the following figures. 1: Baie des  
116 Veys modern site. Arrow: direction of the English Channel current near the shore (Lazure and Desmare, 2012). 2:  
117 Landévennec Medieval site. 3: Riec-sur-Bélon modern site. 4: Charente-Maritime, comprising the modern site of Marennes-  
118 Oléron (A), the Renaissance site of Brouage (B), and the Medieval site of Broue tower (C). Arrow: direction of the current in  
119 the bay (Dechambenoy et al., 1977). 5: Tès modern site. 6: Leucate modern site. 7: Corsica island sites, comprising the  
120 modern site of Diana lagoon (A) and the Antiquity site of Aléria (B). Additional archaeological groups are the Medieval  
121 shells found at La Malène of confirmed Mediterranean origin and two groups unearthed at Cybèle (Lyons) of unknown  
122 origin.

123

## 124 **2.2. Sample selection and preparation**

125 The preparation protocol is given in Mouchi et al. (2020a). Multiple specimens were selected  
126 from each group based on the apparent preservation of the umbo region of the shell. Epibionts, when  
127 present, were mechanically removed. The umbo of the left valve was embedded in Huntsman Araldite  
128 2020 epoxy resin, cut through using a Buehler low-speed saw to expose the preserved internal  
129 structures along the growth axis, and made into polished 750 µm-thick sections. As the umbo records  
130 the entire growth of the shell in a condensed area, geochemical analyses on such sections have the  
131 benefit of being deprived of surface contaminations of chemical or organic origin (Richardson et al.,  
132 1993; Kirby et al., 1998). Indeed, the umbo is a dense area, protected from the exterior environment  
133 within the bivalve, which generally presents a much better preservation compared to the rest of the  
134 shell. In addition, oyster shells are made of lamellae that can be intertwined with empty spaces that can  
135 be filled with organic and sedimentary contaminants, which could strongly interfere with the quality of  
136 the measurements.

137 Each section was observed under cathodoluminescence to ensure the pristine state of the  
138 surface and to outline the seasonal calibration of the shell based on the intensity of luminescence  
139 (Lartaud et al., 2010b; Mouchi et al., 2018; Huygue et al., 2019). Following the growth direction, areas  
140 of strong luminescence correspond to parts of the shell built in summer periods, while areas in dull  
141 luminescence have grown during winter periods. Observations were completed using a Cathodyne-



142 OPEA cold cathode at ISTE<sub>P</sub>, Sorbonne Université (Paris, France) with 15-20 kV, 200-400  $\mu\text{A}\cdot\text{mm}^{-2}$   
143 and a pressure of 0.05 Torr. Shells from Leucate (Cg\_Leu\_M) were the only specimens that did not  
144 exhibit cathodoluminescence, which made the seasonal calibration impossible. The seasonal  
145 calibration from morphology proposed by Kirby et al. (1998) was also unsuccessful due to the absence  
146 of the necessary curved surface of the umbo. All specimens from the other groups were seasonally  
147 calibrated.

### 148 **2.3. Geochemical analyses by LA-ICP-MS**

149 Measurements were performed using an Element XR (ThermoScientific) ICP-MS coupled  
150 with a RESOLUTION 193 nm ArF excimer ablation system equipped with an S155 two-volume ablation  
151 cell (Australian Scientific Instruments) at ISTE (University of Lausanne, Switzerland). The analyses  
152 were carried out with a pulse repetition rate of 20 Hz and an on-sample energy density of 4  $\text{J}\cdot\text{cm}^{-2}$ .  
153 Sample areas were cleaned from potential surface contamination (during polishing) by conducting pre-  
154 ablation. Spot size was 200  $\mu\text{m}$ . Measurements were conducted on both summer and winter zones,  
155 based on the seasonal calibration. Measurements on Leucate specimens (Cg\_Leu\_M) were positioned  
156 randomly instead. Each specimen (shell) was measured several times in order to avoid bias due to  
157 internal variability. We carefully avoided performing measurements in suspicious areas regarding  
158 preservation, based on cathodoluminescence observation. We performed at least two adjacent  
159 measurements for each selected season area, with generally six to eight measurements per shell  
160 (sometimes less, *e.g.* four measurements for some Oe\_MO\_M specimens, due to lower growth rates  
161 restricting the surface available for measurements). For most specimens, three to four successive  
162 season areas were sampled. Prior and following each 15-sample series, NIST SRM 612 was measured  
163 for external calibration. Accuracy of the analyses was checked against measurements of the BCR-2  
164 basalt reference material from USGS according to the GeoReM preferred values (Jochum et al., 2005).  
165 Relative standard deviation for all measured elements range from 1.2 % to 5.8 % (**Supplementary**  
166 **Information 2**). Measured elements were La, Ce, Pr, Nd, Sm, Ti, Cr, Cu, Zn, Sr, Ba, Pb, U, Y, and Ca  
167 as the internal standard. Data reduction was performed using the LAMTRACE software (Jackson,  
168 2008). A total of 472 measurements were acquired.

169           2.4. **Data processing**

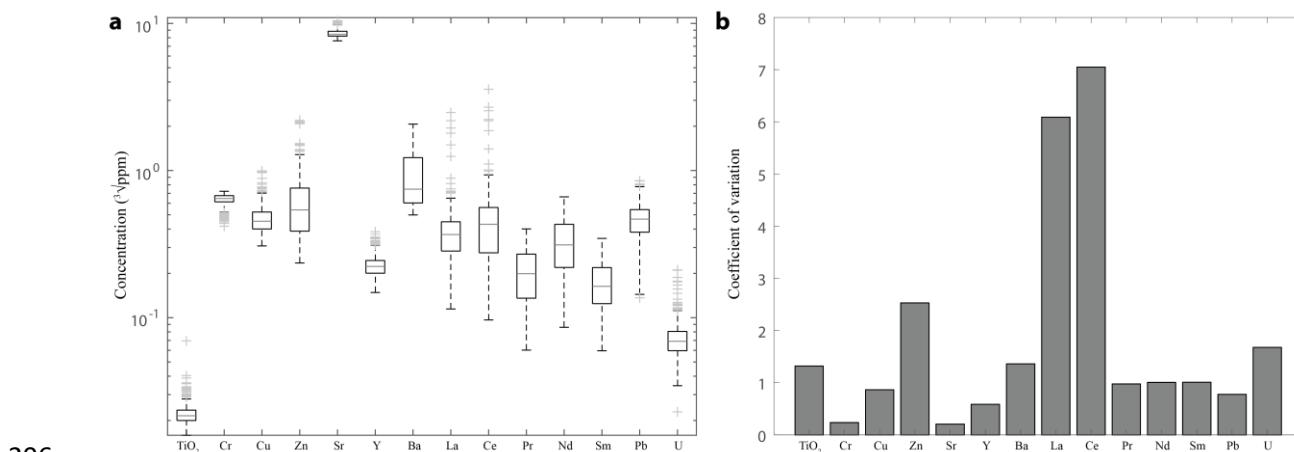
170           All data processing was conducted using the Matlab software (MathWorks,  
171           www.mathworks.com, v. R2017a). As none of the 14 measured elements presented a normal  
172           distribution (Kolmogorov-Smirnov test) due to a right-skewed distribution (towards larger element  
173           abundances), it was necessary to transform the data to normality for statistical processing, which was  
174           performed by using the cubic root transform (Chen and Deo, 2004). Hierarchical cluster analyses were  
175           used to estimate seasonal differences (using the seasonal age models based on the  
176           cathodoluminescence signal) at Baie des Veys on 38 measurements from *C. gigas* specimens  
177           (Cg\_BdV\_M; n=5) and 38 measurements from *O. edulis* specimens (Oe\_BdV\_M; n=5), and at  
178           Marennes-Oléron on 23 measurements from *C. gigas* specimens (Cg\_MO\_M; n=3) and 16  
179           measurements from *O. edulis* specimens (Oe\_MO\_M; n=3). Two methods were tested: unweighted  
180           average distance and “Ward” inner squared distance. The cophenetic correlation coefficient between  
181           the distances obtained from the cluster tree and the original distances (in the multivariate space) is an  
182           indicator of the quality of the estimation (of the hierarchical cluster analysis) to faithfully represent  
183           dissimilarities between observations being compared. Comparison and classification between all  
184           groups were performed using t-SNE (t-distributed Stochastic Neighbour Embedding; van der Maaten  
185           and Hinton, 2008) with the exact Euclidean method. This method allows high-dimensional data points  
186           to be imbedded in low dimensions (typically two dimensions) in a way that respects similarities  
187           between points: distant points in a high-dimensional space correspond to distant embedded low-  
188           dimensional points, and nearby data points in the high-dimensional space correspond to nearby  
189           embedded low-dimensional points (MathWorks, www.mathworks.com, v. R2017a). In other words,  
190           each point represented by t-SNE corresponds to the overall composition of one measurement of all 14  
191           elements, two close points having a similar composition while two distant points reflect different  
192           compositions. To prevent the undesirable over-influence of some elements showing wide variance, we  
193           performed t-SNE on normalized data. The Matlab script for t-SNE processing is available as  
194           **Supplementary Information 3**. As we focus on comparing the concentrations between individual  
195           shells from multiple localities using the same (LA-ICP-MS) analytical method, the host phase (organic

196 or mineral) of specific elements and their resulting co-variations within a measurement are not  
197 discussed here.

198

### 199 3. RESULTS

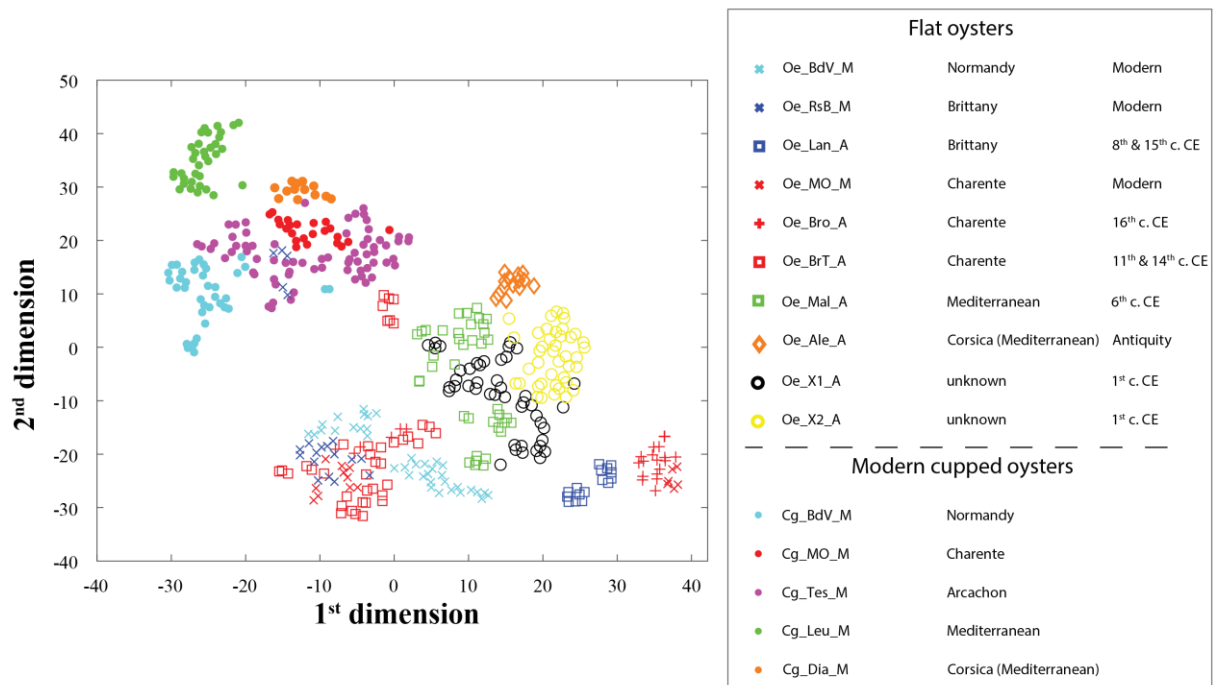
200 All measurement results are presented in **Figure 2a**. The three elements with the largest  
201 coefficients of variation are Ce, La and Zn, followed by U, Ba, and Ti (**Fig. 2b**). All other elements  
202 appear to have a low variance in the dataset. Except for Sr, Ba, Zn, La, and Ce, all measured elements  
203 have concentrations below 1 ppm. Boxplots by element for all the shell groups are provided as  
204 **Supplementary Information 4**. None of the elements can be used to differentiate between the origins  
205 of the various groups on its own.



206  
207 **Figure 2:** Distribution of the 472 measurements for each analyte. **a:** Boxplot with values indicated in cubic root for best  
208 approaching the normality in the distribution and for clarity. Note that the ordinate axis is in logscale. **b:** Coefficient of  
209 variation for each analyte.

210  
211 Similarities and differences between the 15 shell groups based on geochemical data are plotted  
212 in **Figure 3** using t-SNE. First, the five groups of *C. gigas* shells are positioned at the upper left side of  
213 the figure, while *O. edulis* samples are spread out in a much wider area. Moreover, the measurements  
214 performed on both species from the same site (*i.e.*, Cg\_BdV\_M and Oe\_BdV\_M for Baie des Veys,  
215 and Cg\_MO\_M and Oe\_MO\_M for Marennes-Oléron) do not overlap, indicating that the

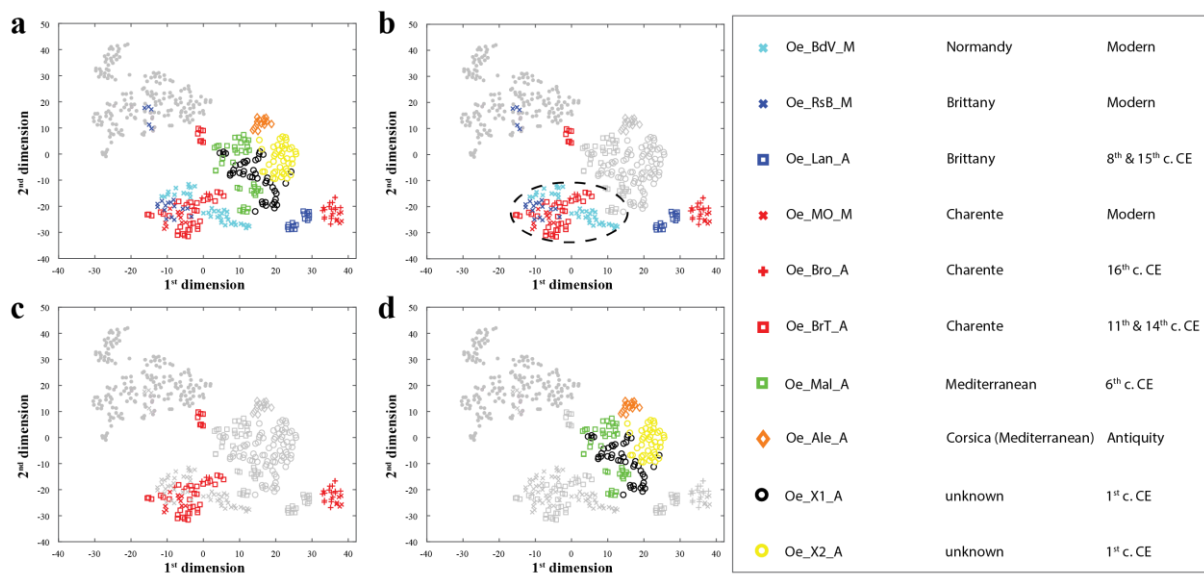
216 compositions of the shells are not identical for both species from the same locality. Furthermore, the  
 217 five groups of *C. gigas* shells are relatively well identified, particularly those of Leucate (Cg\_Leu\_M),  
 218 Diana lagoon (Cg\_Dia\_M) and Baie des Veys (Cg\_BdV\_M). The Marennes-Oléron (Cg\_MO\_M) and  
 219 Tès (Cg\_Tes\_M) groups partially overlap.



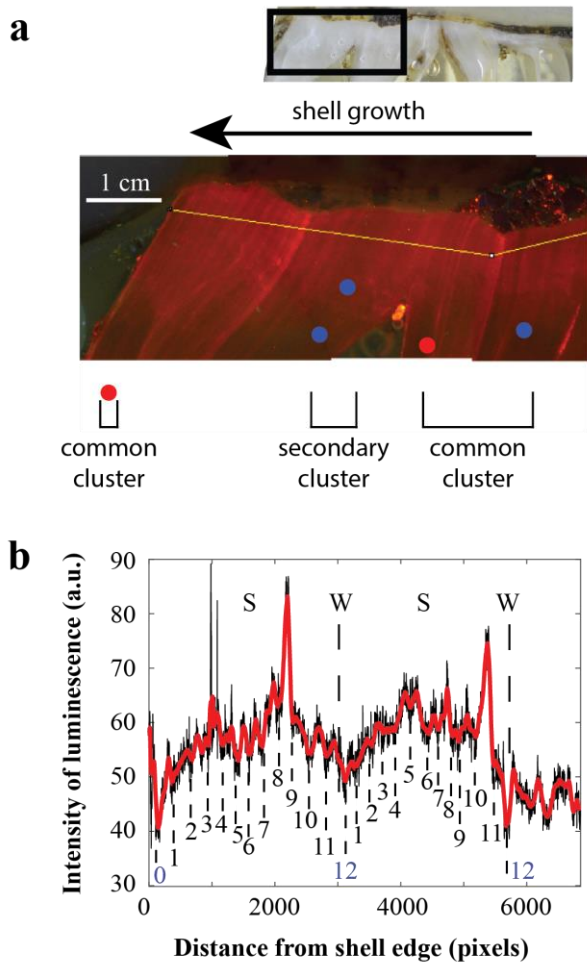
220  
 221 **Figure 3:** Visualization of shell groups' partitioning using t-SNE (exact method using Euclidean distance) based on 472  
 222 measurements. *Crassostrea gigas* shell measurements are indicated with dots. Light blue symbols represent measurements  
 223 from shells originating from Normandy, dark blue symbols represent Brittany, red symbols represent Charente, purple  
 224 symbols represent Arcachon Basin, and green and orange symbols represent the Mediterranean Sea, including Corsica. Two  
 225 groups of Antiquity shells of unknown origin are indicated by yellow and black circles.

226  
 227 Although some *O. edulis* groups are well defined without any measurement overlap from other  
 228 groups (*i.e.*, Oe\_Ale\_A and Oe\_Lan\_A), some groups of this species are more difficult to discriminate  
 229 geochemically (**Figure 4a**). Indeed, when only considering groups originating from localities on the  
 230 English Channel and the Atlantic Ocean coastlines (*i.e.*, open seas with strong tidal influence),  
 231 numerous measurements cluster without discrimination between the locality of origin (dashed ellipse  
 232 in **Figure 4b**). Only the Landévennec (Oe\_Lan\_A) group is absent from this common cluster.  
 233 Inversely, the Oe\_BdV\_M group measurements are found solely in this common cluster. For the

234 Oe\_RsB\_M, Oe\_MO\_M, Oe\_Bro\_A and Oe\_BrT\_A groups, other measurements are found in  
 235 ‘secondary’ clusters in addition to their presence in the common cluster, which are specific to the  
 236 group. Some specimens from these groups have a unique fingerprint corresponding to one or the other  
 237 cluster (common or secondary), while other specimens have fingerprints corresponding to both  
 238 clusters along successive measurements, following shell growth (**Figure 5**). Amongst them,  
 239 Oe\_MO\_M and Oe\_Bro\_A (both from Charente-Maritime) share this ‘secondary cluster’, while Broue  
 240 tower (Oe\_BrT\_A; from the Charente-Maritime region as well) has a ‘secondary cluster’ isolated from  
 241 the others (**Figure 4c**). It is also worth noting that specimens from the Oe\_BrT\_A group, which have  
 242 been collected from two distinct temporal units in the site (see **Supplementary Information 1**),  
 243 present measurements in the common cluster as well as in the secondary cluster for specimens from  
 244 both stratigraphic units (sometimes along the same specimen), confirming that the local elemental  
 245 fingerprint is identical over centuries. However, the two specimens from Landévennec (Oe\_Lan\_A),  
 246 belonging to two different temporal periods, are discriminated from one another by t-SNE (**Figure 3**)  
 247 in the form of two groups of measurements in the Landévennec cluster.



248  
 249 **Figure 4:** Visualization of *O. edulis* shell groups’ partitioning using t-SNE showing specific groups. **a:** t-SNE from Figure 3  
 250 with measurements from *C. gigas* shells shaded. **b:** Same as **a** showing only groups of confirmed English Channel or Atlantic  
 251 Ocean coastlines. The dashed ellipse indicates a cluster common to measurements from several groups. **c:** Same as **a** showing  
 252 only the three Charente groups. **d:** Same as **a** showing only the groups from the Mediterranean coastline and the two groups  
 253 of unknown origin.



254

255 **Figure 5:** Successive measurements along shell growth indicating different fingerprints on specimen 1297-2 from Broue  
 256 tower (Oe\_BrT\_A), namely “common cluster” and “secondary cluster” on Fig. 4b. **a:** Cathodoluminescence view of the last  
 257 two years of growth (corresponding to the area analysed by LA-ICP-MS) on the umbo region and positions of the  
 258 measurements. Red and blue dots correspond to summer and winter measurements, respectively. Note that the first  
 259 measurement on the left is out of the picture frame. **b:** Intensity of luminescence (in arbitrary units) along the umbo following  
 260 the line indicated on **a**, showing the areas of light (corresponding to summers; “S”) and dull (corresponding to winters; “W”)  
 261 luminescence. Smoothing of this signal is shown overlapping in red, and highlights the presence of a monthly tidal cycle  
 262 (numbers).

263 When considering the two remaining groups of confirmed origin, both from the Mediterranean  
 264 Sea (an enclosed basin with a narrow opening to the Atlantic Ocean through the Strait of Gibraltar),  
 265 each group is defined by a single cluster without any overlap (in green and orange in **Figure 4d**). The  
 266 measurements from the groups of unknown origin overlap at least partially with the Oe\_Mal\_A group.

267 Data collected from specimens bred at Baie des Veys and Marennes-Oléron were used to  
268 study the differences between seasons for both species based on dendrograms (**Supplementary**  
269 **Information 5**). Seasons cannot be reliably discriminated, as indicated by the cluster analyses that  
270 show both seasonal measurements mixed together. For Cg\_BdV\_M, the cophenetic correlation  
271 coefficients are 0.80 and 0.52 for average and Ward methods, respectively. In the same site, for  
272 Oe\_BdV\_M, coefficients are 0.89 and 0.77 for average and Ward methods, respectively. Similar  
273 cophenetic correlation coefficients are found for Cg\_MO\_M with 0.70 and 0.62 for average and Ward  
274 methods, respectively, and for Oe\_MO\_M with 0.89 and 0.77 for average and Ward methods,  
275 respectively. The identification of seasons for all the measurements (except Leucate specimens; see  
276 section 2.2) in the t-SNE distribution is also reported in **Supplementary Information 5**.

277

## 278 4. DISCUSSION

### 279 **4.1. Large-scale provenance discrimination**

280 It was previously reported that REE and Y cannot be used for *O. edulis* as a provenance proxy  
281 due to vital effects, unlike *C. gigas* (Mouchi et al., 2020a). Consequently, other elements were  
282 investigated in this study in order to provide a potential regional fingerprint for this species and to find  
283 a way to efficiently compare measurements from *O. edulis* and *C. gigas* in terms of sourcing. The  
284 results show that REE are not the only elements whose incorporation differ between these two species.  
285 Indeed, the Cg\_BdV\_M and Oe\_BdV\_M groups, which originate from the same modern locality (and  
286 reared simultaneously on the same culture table in Baie des Veys, Normandy), exhibit obvious  
287 different compositions (**Figure 3**). Observations are similar for Cg\_MO\_M and Oe\_MO\_M from  
288 Marennes-Oléron, Charente-Maritime. However, it seems possible, when considering only one of the  
289 two species, to discriminate the composition depending on their region of origin, if not the locality.

290 For *C. gigas* specimens, the shells from the Mediterranean Sea (Cg\_Leu\_M and Cg\_Dia\_M),  
291 seem to be separated by t-SNE from the Atlantic Ocean/English Channel groups along the second  
292 dimension (approximately around unit 25 in **Figure 3**). This separation appears to be controlled by a

293 lower abundance in light REE in the Mediterranean groups compared to the Atlantic groups  
294 (**Supplementary Information 4**). This low abundance in light REE can either be specific to the  
295 Mediterranean shells or to the relatively small watersheds from these two localities (the smallest of the  
296 entire dataset). Although most of the Baie des Veys measurements are discriminated by t-SNE from  
297 other groups, some measurements share their composition with a part of the Tès group (Cg\_Tes\_M),  
298 which itself is partially connected to the Marennes-Oléron group (Cg\_MO\_M). This observation tends  
299 to indicate that specimens from the English Channel (Baie des Veys) and the Atlantic Ocean  
300 (Marennes-Oléron and Tès) exhibit some similarities in their geochemical composition.

301 For *O. edulis*, the common cluster (dashed ellipse in **Figure 4b**) gathers measurements from  
302 specimens from the Atlantic Ocean and English Channel coastlines, covering roughly 700 km of  
303 coastline (**Figure 1**) from Charente-Maritime in the south (Oe\_MO\_M, Oe\_Bro\_A, Oe\_BrT\_A) to  
304 Normandy in the north (Oe\_BdV\_M). As the English Channel and the Atlantic Ocean are connected  
305 across a wide area, the overall composition of seawater should share some similarities. On the  
306 contrary, the Mediterranean Sea is a semi-enclosed basin and is recharged by the Atlantic Ocean  
307 through the narrow Strait of Gibraltar. A difference in composition is expected in shells from  
308 Mediterranean localities. In addition, the near absence of tidal range in this region compared to the  
309 Atlantic Ocean can cause differences in fluid mixing and elemental incorporation in the shells.  
310 Therefore, it appears possible to discriminate, at a large scale, between specimens from the Atlantic  
311 Ocean/English Channel and the Mediterranean Sea.

#### 312 **4.2. Fine-scale provenance discrimination**

313 The common cluster composed of samples from Oe\_BdV\_M, Oe\_RsB\_M, Oe\_MO\_M,  
314 Oe\_Bro\_A, and Oe\_BrT\_A shells (Baie des Veys: Normandy; Riec-sur-Belon: Brittany; Marennes-  
315 Oléron, Brouage and Broue tower: Charente) represents a homogenous fingerprint. These groups are  
316 from watersheds with quite distinct geological formations (limestones, basalts, etc...) but share a large  
317 seawater body (*i.e.*, the Atlantic Ocean). However, we observe that each group in this cluster has also  
318 a secondary cluster outside the common one, which seems group-specific, except for the Baie des  
319 Veys (Oe\_BdV\_M; **Figure 4b**). Within these groups, some specimens have all their measurements



320 within a single cluster (either the common cluster or the secondary cluster of the corresponding  
321 group), while other specimens have some measurements in both clusters (**Figure 5**). As these  
322 specimens have not been transferred from one location to another during growth, it appears that these  
323 changes in elemental incorporation occurred over the growth of the organism in the same site. As  
324 these changes occur multiple times over the growth period (**Figure 5**), it cannot be caused by  
325 ontogeny. This cyclical pattern is not linked to seasonality (this was checked by the seasonal  
326 calibration using cathodoluminescence; see t-SNE figure in **Supplementary Information 5**).  
327 Consequently, a different factor is at play. Temporal resolution of the LA-ICP-MS measurements is  
328 approximately one month, based on a tidal cathodoluminescence signal (Mouchi et al., 2013; see  
329 monthly cycles on **Figure 5b**) and *in vivo* labelling (Lartaud et al., 2010b; **Supplementary**  
330 **Information 6**). Growth rates can however be different according to the specimen and the period  
331 considered, and some measurements may represent a slightly shorter or longer period (Huyghe et al.,  
332 2019). Since all the corresponding groups originate from the English Channel and the Atlantic Ocean  
333 shorelines, tidal influence can be a pertinent factor. Indeed, all the groups from the Mediterranean Sea  
334 (Oe\_Mal\_A, Oe\_Ale\_A), which exhibits a very weak tidal range (only a few centimetres), are  
335 excluded from the common cluster (**Figure 4d**). In localities with a broad tidal range, the influence of  
336 the chemistry of nearby rivers could fluctuate widely, increasing during low tide and, on the contrary,  
337 being diluted with seawater at high tide. If this were the case, the secondary clusters would represent  
338 the correct local fingerprint, while the common cluster would correspond to the fingerprint of Atlantic  
339 seawater. Manganese is known to fluctuate in oyster shells from ebb to flood currents (Huyghe et al.,  
340 2019). Other chemical elements (*e.g.* those measured here) could present similar fluctuations.  
341 Switching between these two compositions, which are responsible for the presence of two distinct  
342 fingerprints, could be caused by the relative proportion (by volume in the analysed shell) of carbonate  
343 formed during ebb and flow currents. The proportion may vary, depending on growth rates. The case  
344 of the Baie des Veys shells (Oe\_BdV\_M group) is singular as it has no secondary cluster (**Figure 4b**).  
345 Interestingly, this site is also the locality with the most open marine settings from all modern groups.  
346 Although some shells of other groups did not have measurements corresponding to secondary clusters,  
347 the fact that no measurements from the 38 performed on five specimens are outside this common

348 cluster would tend to imply that there is only one fingerprint in this site. This observation is supported  
349 by the marine water mass current of the Baie des Veys, which flows towards the direction of the  
350 rivers' outputs from the locality where the oysters were collected (**Figure 1**; Lazure and Desmare,  
351 2012), hence limiting the influence of the composition of the freshwater coming from the land. Becker  
352 et al. (2005) measured the elemental fingerprint of young mussel shells in several localities in San  
353 Diego County to study the larval dispersal along the coastline. They were able to observe distinct  
354 fingerprints for specimens from estuarine locations, but could not clearly discriminate open marine  
355 locations. We suspect this is what is observed here, with a 'marine' fingerprint common to several  
356 groups (being identical to that of an open marine locality, *i.e.* Baie des Veys), and a secondary  
357 fingerprint, specific to the locality, in environments where continental inputs are sufficiently strong.  
358 This assumption is supported by a higher and more stable salinity in Baie des Veys (approximately 33  
359 all year) than in Marennes-Oléron (27 to 34; Lartaud et al., 2010c).

360 Temporal changes in the local elemental fingerprint have already been reported in mollusc  
361 shells, such as *Cerastoderma edule* and *Mytilus edulis* from Ireland (Ricardo et al., 2017; Bennion et  
362 al., 2019). These differences occur within months and observations in this study confirm that it is also  
363 the case for *O. edulis*, although the same is not true for *C. gigas*. These differences appear to switch  
364 back and forth between two fingerprints (**Figure 5**), one being common to multiple groups of shells of  
365 various origins in the French Atlantic Ocean and English Channel coastlines.

366 The case of the Charente-Maritime groups (Marennes-Oléron: Oe\_MO\_M; Brouage:  
367 Oe\_Bro\_A; and Broue tower: Oe\_BrT\_A) is interesting, as two distinct secondary clusters are visible  
368 in the t-SNE plot (**Figure 4c**). One of these groups of shells has been collected in the present day  
369 (Marennes-Oléron) with the exact location known, while the two other groups (Brouage and Broue  
370 tower) have been found in archaeological sites on land, with evidence that these locations were on the  
371 shoreline at the corresponding ages of the specimens. The fingerprint of the modern group is shared by  
372 the Brouage group dated from the 16<sup>th</sup> century CE (Oe\_Bro\_A). On the contrary, the Broue tower  
373 shells from the 11<sup>th</sup> and the 14<sup>th</sup> centuries CE (Oe\_BrT\_A) present a distinct fingerprint. It may be  
374 possible that the oysters from this group were living in a locality in the region under the influence of

375 another freshwater flow with a different water composition. Indeed, the Marennes-Oléron bay has two  
376 major tributary rivers, which cross different geological formations, although the main rock type is  
377 limestone (Bourgueil et al., 1968, 1972; Platel et al., 1977, 1978; Bambier et al., 1982; Hanztpergue et  
378 al., 1984; Mourier et al., 1989). The site of Brouage, from which were unearthed the shells of the  
379 Oe\_Bro\_A group, is located at the same level in the bay as the modern Marennes-Oléron group  
380 (Oe\_MO\_M; Champagne et al. 2012; **Figure 1**), with which it shares its secondary cluster. The site of  
381 the Broue tower, where the shells from the Oe\_BrT\_A group were discovered, is located further south,  
382 near the current output of the Seudre river (**Figure 1**; Normand et al., 2019). As seawater currents  
383 cross the bay from north to south, the oysters from the Oe\_MO\_M and Oe\_Bro\_A groups must have  
384 been under the influence of the Charente River (north side of the bay), but not the Seudre River. On  
385 the contrary, specimens from the Oe\_BrT\_A group must have been mainly under the influence of the  
386 Seudre River. The measurements show that, in such contexts, the identification of the region can be  
387 narrowed down to the watershed level. In addition to this, although temporal differences in local  
388 elemental fingerprints have been reported in other regions (Ricardo et al., 2017; Bennion et al., 2019),  
389 the fact that both modern (Oe\_MO\_M) and ancient (Renaissance, Oe\_Bro\_A) shells share a common  
390 cluster and a local cluster over the course of several centuries indicate that multiple measurements  
391 over the growth direction of shells can allow the local elemental fingerprint to be recognized, whatever  
392 the period of collection. This interpretation is also supported by the Oe\_BrT\_A specimens, which  
393 present fingerprints corresponding to both the common cluster and the same (locality-specific)  
394 secondary cluster, whether specimens are from the 11<sup>th</sup> or the 14<sup>th</sup> c. CE.

395 The only group of shells from the English Channel/Atlantic Ocean coastline that have no  
396 measurements corresponding to the common cluster is Oe\_Lan\_A. The Medieval site at Landévennec,  
397 from which these shells were unearthed, is located in the direct proximity of the Aulne River (**Figure**  
398 **1**). Although the salinity is close to marine (generally around 32 except during flooding events where  
399 salinity drops to 15; Monbet and Bassoulet, 1989), the river rate of flow (annual mean of 24 m<sup>3</sup>.s<sup>-1</sup>;  
400 Auffret, 1981) is probably high enough to induce a strong influence in terms of chemical composition  
401 of the local seawater. That way, even at high tide, the composition of shells, derived from the local

402 seawater, would still be substantially influenced from the Aulne River. The two sub-groups from this  
403 cluster, with each corresponding to one specimen of different age (8<sup>th</sup> and 15<sup>th</sup> centuries CE), are  
404 probably due to a different degree of the influence of freshwater input. As several centuries separate  
405 these specimens, it is probable that the local geomorphology and water level changed, causing  
406 relocation of the supply of oysters from the inhabitants. Nevertheless, the close similar fingerprint of  
407 these specimens implies that they originate from nearby locations.

408 For *C. gigas* groups, all measurements from the Cg\_Leu\_M group of shells are clustered away  
409 from the other groups in **Figure 3**, with highly negative values on the 1<sup>st</sup> dimension axis and highly  
410 positive values on the 2<sup>nd</sup> dimension axis. This observation indicates that the elemental compositions  
411 of these shells are substantially different than the shells from the other regions. The fingerprint from  
412 the Diana lagoon (Cg\_Dia\_M) is also easily discriminated from the others. Compared to the other  
413 regions, these localities are characterized by small watersheds, uniquely consisting in limestone. As  
414 one can expect a smaller surface exposed to weathering than those of the other studied localities, the  
415 abundance of some elements in the shell should be lower at Leucate and Diana lagoon. Indeed, both  
416 groups are characterized by low abundances of light REE compared to the other groups, but the other  
417 analysed elements do not present such a systematic lower content (**Supplementary Information 4**). It  
418 is also possible that, as both these localities are in restricted lagoons, salinity can be at play. Indeed,  
419 Diana Lagoon (Mediterranean Sea) is known to have a high salinity (37.3 annual mean; Orsini et al.,  
420 2001) and Leucate lagoon has a seasonally dominated salinity (26 in winter and 42 in summer due to  
421 evaporation; Andrisoa et al., 2019), whereas Baie des Veys and Marennes-Oléron (Atlantic coastline)  
422 have lower salinities (33.4 and 32.4 annual mean, respectively; Lartaud et al., 2010c).

423 For “Atlantic Ocean” *C. gigas* specimens, the Baie des Veys group (Cg\_BdV\_M; although  
424 situated in the English Channel, with a wide access to the Ocean) appears to be the most distinct by t-  
425 SNE between these groups, with only some measurements overlapping with the Tès group. This is  
426 interesting, as *O. edulis* shells from the same locality (Oe\_BdV\_M) had the peculiar characteristic of  
427 representing the composition of a cluster common to other Atlantic groups. The Tès (Cg\_Tes\_M) and  
428 Marennes-Oléron (Cg\_MO\_M) groups share their distribution in the t-SNE graph, with the Marennes-

429 Oléron distribution entirely comprised into a restricted portion of the Tès distribution. The large  
430 distribution by t-SNE of Tès measurements compared to Marennes-Oléron can be explained by the  
431 annual range of salinity (approx. 15 and 5, respectively for Tès and Marennes-Oléron; Lartaud et al.,  
432 2010c). These two localities (Arcachon Basin and Charente-Maritime) have their watersheds crossing  
433 different geological formations with mainly Cenozoic river deposits for Tès (Dubreuilh et al., 1992)  
434 and mainly Mesozoic limestone for Marennes-Oléron (Bourgueil and Moreau, 1967, 1970; Bourgueil  
435 et al., 1968; Platel et al., 1977; 1978). Still, the deposit cover of the respective watersheds does not  
436 appear to be sufficient to entirely discriminate these groups.

#### 437 **4.3. Attempting to identify the provenance of the Lyons/Cybèle shells**

438 The Oe\_Mal\_A group from La Malène belongs to a specific locality, which is unknown, but at  
439 least confirmed from the Mediterranean coastline, probably from Languedoc coastline due to the  
440 associated remains from other taxa specific to Roman-influenced Languedoc customs (Bardot-Cambot  
441 and Forest, 2014; Forest, 2019; Forest, 2020 for Mureau, 2020). Measurements from this group are  
442 discriminated from the other *O. edulis* groups of known origins (all from the Atlantic Ocean/English  
443 Channel coastlines) and these groups are relatively close to one another. We note that the Oe\_X1\_A  
444 and Oe\_X2\_A group distributions are partially overlapping (**Figure 4d**). It seems that the shells from  
445 these groups of unknown origin, and found at the Antiquity Cybèle site (Lyons, over 200 km away  
446 from the nearest shore), share part of their fingerprint, which could imply that all these specimens  
447 lived in the same geographic region, yet not the exact same locality. Therefore, although geochemistry  
448 confirms that the Cybèle groups initially determined by morphometric parameters (Bardot-Cambot,  
449 2013) do exist, our data tend to discard the hypothesis that one group originated from the  
450 Mediterranean Sea and the other from the Atlantic Ocean. Although additional sites from both Atlantic  
451 and Mediterranean shorelines would be required to affirm this, it seems here that populations from  
452 these groups lived a short distance away from each other, and the fingerprint of the Oe\_X1\_A group  
453 seems to correspond to that of La Malène specimens (Oe\_Mal\_A). If true, additional specimens in  
454 other localities on the Mediterranean shoreline should be analysed to identify their locality of origin,  
455 but at the moment, we were not able to collect wild modern specimens.

#### 456 **4.4. Quality of the discrimination method**

457 As our dataset is constituted of 14 elements per measurement, attempts were made to reduce  
458 this number for ease of analytical and data processing work. Some elements were found to be of  
459 increased importance compared to others to adequately separate measurements from different groups  
460 using t-SNE. By successive removal of one element from the dataset, Pb, Ba and U are the most  
461 effective at successfully discriminating *O. edulis* groups from the Mediterranean Sea and the Atlantic  
462 Ocean (**Supplementary Information 7**). Rare Earth Elements (La, Ce, Pr, Nd, Sm), as found by  
463 Mouchi et al. (2020a), were most useful for discriminating *C. gigas* groups. All other elements were  
464 found to contribute equally to discriminating specific localities. In the end, the removal of any of the  
465 measured elements systematically reduces the quality of the discriminating method.

466 Cross-validation of the clusters was attempted on *O. edulis* measurements (without the groups  
467 of unknown origin, *i.e.* Oe\_X1\_A and Oe\_X2\_A) using discriminant analysis. We obtained a cross-  
468 validated classification error of 24.3% (out of 210 measurements). However, when we removed all  
469 measurements from the common cluster (putatively corresponding to the open marine fingerprint,  
470 including all measurements from the Oe\_BdV\_M group) from the comparative dataset, we obtained a  
471 cross-validated classification error of 0.8% (out of 123 measurements from 7 groups). Becker et al.  
472 (2005) were able to retrieve an open marine origin from San Diego County mussel shell composition  
473 with a 5% error (out of 41 measurements), which corresponded to misclassification to open bays.  
474 However, although these specimens had been collected from six open marine localities along the  
475 Pacific Ocean coastline of San Diego, the correct identification of the site had a 44 % error.  
476 Misclassification of specimens from two open bays (between both bays and all open marine localities  
477 as a whole) presented errors of 33 and 62 % (out of 6 and 8 measurements, respectively) due to a  
478 misclassification of measurements to open marine environments. These results indicated that the open  
479 marine fingerprint from the mussel shell composition is similar along 50 km of coastline (range of the  
480 collection sites of the study), and that elemental fingerprinting of specimens from intertidal localities  
481 in bays present some similarities to the regional open marine fingerprint. Our observations concur with  
482 these conclusions, albeit with additional precision.

483

## 484 5. CONCLUSION

485 Previous attempts to discover the geographical origin of archaeological oyster shells based on  
486 geochemistry presented various degrees of success due to the use of isotopic ratios that are strongly  
487 influenced by local environmental conditions, which can be similar over extremely remote areas. In  
488 this study, elemental fingerprinting of oyster shells from 15 different groups was used, highlighting  
489 several points. First, different elemental incorporation behaviours prevent the direct comparison of  
490 different species. Second, cluster analysis from the t-SNE method suggests that a regional fingerprint  
491 seems to exist and to be distinguishable from large water bodies (seas and oceans). Third, in  
492 environments with restricted influence of oceanic water, a more precise fingerprint is identified and  
493 the locality (at the watershed scale) can be found. In addition, as previous studies reported, none of the  
494 elements is able to differentiate between the origins of various groups on its own. Last but not least,  
495 this technique was successful to identify the provenance of oyster shells of known and previously  
496 unknown origin from archaeological sites. Therefore, this technique appears adequate and promising  
497 to pinpoint the provenance of oyster shells. It remains necessary, however, to have the elemental  
498 fingerprint of a multitude of coastal sites as a database, so that the fingerprint of unknown specimens  
499 can be recognized.

500

## 501 6. ACKNOWLEDGEMENTS

502 This work was carried out by the support of the TracOstrea project, funded by the  
503 Collaborative Research Project “*Les Marais Charentais au Moyen-Âge et à l’époque moderne*” and  
504 the University of Rennes 1. The authors would like to thank Frédéric Delbès and Mikaël Guiavarch for  
505 the work they performed on the preparation of the thin sections. We thank Michel Ropert from the  
506 marine station of Port-en-Bessin (IFREMER), Philippe Geairon from the marine station of La  
507 Tremblade (IFREMER) and Danièle Maurer from the marine station of Arcachon (IFREMER) for  
508 their precious help in the breeding of oysters at Baie des Veys, Marennes-Oléron and Tès localities,

509 respectively. The authors would like to acknowledge three anonymous reviewers for their proposed  
510 improvements of the manuscript and Karin Verrecchia for editing the English.

511

## 512 7. Data availability

513 The data used in this study have been deposited in the Zenodo data repository  
514 (<http://doi.org/10.5281/zenodo.4681223>; Mouchi et al., 2021).

515

516 Declarations of interest: none.

517

## 518 REFERENCES

519 André, J., 1981. L'alimentation et la cuisine à Rome. *Les Belles Lettres*, Paris, 264 p.

520 Andrews, A.C., 1948. Oysters as a food in Greece and Rome. *The Classical Journal*, XLIII,  
521 299-303.

522 Andrisoa, A., Lartaud, F., Rodella, V., Neveu, I., Stieglitz, T.C., 2019. Enhanced growth rates  
523 of the Mediterranean mussel in a coastal lagoon driven by groundwater inflow. *Frontiers in Marine*  
524 *Science*, 6, 753. doi: <https://doi.org/10.3389/fmars.2019.00753>.

525 Apolinarska, K., Kurzawska, A., 2020. Can stable isotopes of carbon and oxygen be used to  
526 determine the origin of freshwater shells used in Neolithic ornaments from Central Europe?  
527 *Archaeological and Anthropological Sciences*, 12, 15. doi: [https://doi.org/10.1007/s12520-019-00978-](https://doi.org/10.1007/s12520-019-00978-2)  
528 [2](https://doi.org/10.1007/s12520-019-00978-2).

529 Auffret, G., 1981. Dynamique sédimentaire de la marge continentale celtique. *Ph.D. thesis*,  
530 Université de Bordeaux I.

531 Bajnóczi, B., Schöll-Barna, G., Kalicz, N., Siklósi, Z., Hourmouziadis, G.H., Ifantidis, F.,  
532 Kyparissi-Apostolika, A., Pappa, M., Veropoulidou, R., Ziota, C., 2013. Tracing the source of Late



533 Neolithic *Spondylus* shell ornaments by stable isotope geochemistry and cathodoluminescence  
534 microscopy. *Journal of Archaeological Science*, 40, 874-882. doi: 10.1016/j.jas.2012.09.022.

535 Bambier, A., Capdeville, J.-P., Cariou, E., Floc'h, J.-P., Gabilly, J., Hantzpergue, P., 1982.  
536 Notice explicative, Carte géol. France (1/50 000), feuille La Rochefoucauld (686). Orléans: BRGM,  
537 30 p, Carte géologique par A. Bambier et al., 1982.

538 Bardot-Cambot, A., 2013. Les coquillages marins en Gaule romaine. Approche socio-  
539 économique et socio-culturelle. *BAR International Series*, 2481, Archaeopress, Oxford, 270 p.

540 Bardot-Cambot, A., 2014. Consommer dans les campagnes de la Gaule Romaine. *Revue du*  
541 *Nord*, 21, Hors-série, Collection Art et Archéologie, 109-123.

542 Bardot-Cambot, A. Forest, V., 2014. Une histoire languedocienne des coquillages marins  
543 consommés, du Mésolithique à nos jours. *In*: Costamagno S. (Ed.) Histoire de l'alimentation humaine  
544 : entre choix et contraintes. *Actes du 138<sup>e</sup> congrès national des sociétés historiques et scientifiques*  
545 (Rennes, 2013). Actes des congrès nationaux des sociétés historiques et scientifiques. Édition  
546 électronique, p. 88-104.

547 Bayne, B.L., Ahrens, M., Allen, S.K., Anglès D'auriac, M., Backeljau, T., Beninger, P., Bohn,  
548 R., Boudry, P., Davis, J., Green, T., Guo, X., Hedgecock, D., Ibarra, A., Kingsley-Smith, P., Krause,  
549 M., Langdon, C., Lapègue, S., Li, C., Manahan, D., Mann, R., Perez-Paralle, L., Powell, E.N.,  
550 Rawson, P.D., Speiser, D., Sanchez, J.-L., Shumway, S., Wang, H., 2017. The proposed dropping of  
551 the genus *Crassostrea* for all Pacific cupped oysters and its replacement by a new genus *Magallana*: A  
552 dissenting view. *Journal of Shellfish Research*, 36, 545-547. doi: 10.2983/035.036.0301.

553 Becker, B.J., Fodrie, F.J., McMillan, P.A., Levin, L.A., 2005. Spatial and temporal variation in  
554 trace elemental fingerprints of mytilid mussel shells: A precursor to invertebrate larval tracking.  
555 *Limnology and Oceanography*, 50, 48-61.

556           Bennion, M., Morrison, L., Brophy, D., Carlsson, J., Cortiñas Abrahantes, J., Graham, C.T.,  
557 2019. Trace element fingerprinting of blue mussel (*Mytilus edulis*) shells and soft tissues successfully  
558 reveals harvesting locations. *Science of the Total Environment*, 685, 50-58.

559           Bourgueil, B., Moreau, P., 1967. Notice explicative, Carte géol. France (1/50 000), feuille  
560 Cognac (708). Orléans, BRGM, 12 p., Carte géologique par B. Bourgueil et P. Moreau.

561           Bourgueil, B., Moreau, P., 1970. Notice explicative, Carte géol. France (1/50 000), feuille  
562 Angoulême (709). Orléans, BRGM, 20 p., Carte géologique par B. Bourgueil et P. Moreau.

563           Bourgueil, B., Moreau, P., Vouve, J., 1968. Notice explicative, Carte géol. France (1/50 000),  
564 feuille Saintes (683). Orléans: BRGM, 19 p, Carte géologique par B. Bourgueil et al., 1968.

565           Bourgueil, B., Moreau, P., Gabet, C., L'Homer, A., Vouve, J., 1972. Notice explicative, Carte  
566 géol. France (1/50 000), feuille Rochefort (658). Orléans: BRGM, 30 p, Carte géologique par B.  
567 Bourgueil et al., 1972.

568           Campbell, G., 2010. Oysters ancient and modern: potential shape variation with habitat in flat  
569 oysters (*Ostrea edulis* L.), and its possible use in archaeology, *Munibe*, Sup. 31, 176-187.

570           Carson, H.S., 2010. Population connectivity of the Olympia oyster in Southern California.  
571 *Limnology and Oceanography*, 55, 134-148.

572           Champagne, A., Aoustin, D., Dupont, C., 2012. La citadelle de Brouage et la dynamique  
573 paléoenvironnementale du marais charentais : l'apport de la malacologie et de la palynologie. *Bilan*  
574 *Scientifique Régional 2011 de Poitou-Charentes, Service Régional de l'Archéologie*. Poitiers, 294-303.

575           Chaufourier, G., Busson, D., Dupont, C., 2015. Provenance des huîtres consommées à Lutèce  
576 à la fin de la période Augustéenne. *Revue Archéologique d'Île-de-France*, 7-8, 217-229.

577           Chen, W.W. Deo, R.S., 2004. Power transformations to induce normality and their  
578 applications. *Journal of the Royal Statistical Society Series B*, 66, 117-130.

579 Craig, H. 1965. The measurement of oxygen isotope palaeotemperatures. *In*: Tongiorni, E (ed.),  
580 Stable isotopes in oceanographic studies and palaeotemperatures, 161–182. Pisa: Consiglio Nazionale  
581 delle Ricerche Laboratorio di Geologia Nucleare.

582 Dechambenoy, C.L., Pontier, F., Sirou, F., Vouvé, J., 1977. Apport de la thermographie  
583 infrarouge aéroportée à la connaissance de la dynamique superficielle des estuaires (système Charente-  
584 Seudre-Anse de l'Aiguillon). *Comptes Rendus de l'Académie des Sciences de Paris*, 284, 1269-1272.

585 Dubreuilh, J., Karnay, G., Bouchet, J.-M., Le Nindre, Y.-M., 1992. Notice explicative, Carte  
586 géol. France (1/50 000), feuille Arcachon (825). Orléans, BRGM, 53 p., Carte géologique par J.  
587 Dubreuilh, J.-M. Bouchet.

588 Dupont, C., 2016. Could occupation duration be related to the diversity of faunal remains in  
589 Mesolithic shell middens along the European Atlantic seaboard? *Quaternary International*, 407, 145-  
590 153. doi : 10.1016/j.quaint.2016.01.039.

591 Durham, S.R., Gillikin, D.P., Goodwin, D.H., Dietl, G.P., 2017. Rapid determination of oyster  
592 lifespans and growth rates using LA-ICP-MS line scans of shell Mg/Ca ratios. *Palaeogeography*,  
593 *Palaeoclimatology, Palaeoecology*, 485, 201-209. Doi: 10.1016/j.palaeo.2017.06.013.

594 Eerkens, J.W., Herbert, G.S., Rosenthal, J.S., Spero, H.J., 2005. Provenance analysis of  
595 *Olivella biplicata* shell beads from the California and Oregon Coast by stable isotope fingerprinting.  
596 *Journal of Archaeological Science*, 32, 1501-1514.

597 Eerkens, J.W., Rosenthal, J.S., Stevens, N.E., Cannon, A., Brown, E.L., Spero, H.J., 2010.  
598 Stable isotope provenance analysis of *Olivella* shell beads from the Los Angeles Basin and San  
599 Nicolas Island. *Journal of Island & Coastal Archaeology*, 5, 105-119. Doi:  
600 10.1080/15564890902955327.

601 Fodrie, F.J., Becker, B.J., Levin, L.A., Gruenthal, K., McMillan, P.A., 2011. Connectivity  
602 clues from short-term variability in settlement and geochemical tags of mytilid mussels. *Journal of*  
603 *Sea Research*, 65, 141-151.

604 Forest, V., 2019. Les paysans consommateurs et les vestiges fauniques archéologiques : une  
605 fausse évidence. In: G. Ferrand, J. Petrowiste (Eds.) Le nécessaire et le superflu. Le paysan  
606 consommateur. *Actes des XXXVI<sup>e</sup> Journées internationales d'histoire de l'Abbaye de Flaran*, October  
607 17<sup>th</sup>-18<sup>th</sup> 2014, Presses Universitaires du Midi, Toulouse, pp.69-78.

608 Forest, V., 2020. Étude archéozoologique préliminaire : conchyliologie. La Malène – Les  
609 Piboulèdes (Lozère) (périodes antique et médiévale). Rapport inédit.

610 Gruet, Y., Prigent, D., 1986a. Etude de deux prélèvements d'huîtres d'époque gallo-romaine  
611 provenant d'Alet (Saint-Malo). *Les Dossiers du CeRAA*, 14, 123-129.

612 Gruet, Y., Prigent, D., 1986b. Les buttes de Saint-Michel-en-l'Herm (Vendée) : caractères de  
613 la population d'huîtres (*Ostrea edulis* Linné) et de sa faune associée. *Haliotis*, 15, 3-16.

614 Hantzpergue, P., Bonnin, J., Cariou, E., Gomez de Soto, J., Moreau, P., 1984. Notice  
615 explicative, Carte géol. France (1/50 000), feuille Mansle (685). Orléans: BRGM, 24 p, Carte  
616 géologique par P. Hantzpergue et al., 1984.

617 Herz, N., Waelkens, M., 1988. Classical marble: Geochemistry, Technology, Trade. Springer-  
618 Science + Business Media, SV, 464 p.

619 Huyghe, D., de Rafelis, M., Ropert, M., Mouchi, V., Emmanuel, L., Renard, M., Lartaud, F.,  
620 2019. New insights into oyster high-resolution hinge growth patterns. *Marine Biology*, 166, 48.

621 Huyghe, D., Emmanuel, L., de Rafelis, M., Renard, M., Ropert, M., Labourdette, N., Lartaud,  
622 F., 2020. Oxygen isotope disequilibrium in the juvenile portion of oyster shells biases seawater  
623 temperature reconstructions. *Estuarine, Coastal and Shelf Science*, 240, 106777.

624 Jackson, S.E., 2008. LAMTRACE data reduction software for LA-ICP-MS. In: Laser ablation  
625 ICP-MS in the Earth sciences: Current practices and outstanding issues. *The Canadian Mineralogist*,  
626 40, 305-307.

627 Jochum, K.P., Nohl, U., Herwig, K., Lammel, E., Stoll, B., Hofmann, A.W., 2005. GeoReM:  
628 A new Geochemical database for reference materials and isotopic standards. *Geostandards and*  
629 *Geoanalytical Research*, 29, 333-338, doi 10.1111/j.1751-908X.2005.tb00904.x.

630 Kirby, M.X., Soniat, T.M., Spero, H.J., 1998. Stable isotope sclerochronology of Pleistocene  
631 and recent oyster shells (*Crassostrea virginica*). *Palaios*, 13, 560–569.

632 Kuzmin, Y.V., Alekseyev, A.N., Dyakonov, V.M., Grebennikov, A.V., Glascock, M.D., 2018.  
633 Determination of the source for prehistoric obsidian artifacts from the lower reaches of Kolyma River,  
634 Northeastern Siberia, Russia, and its wider implications. *Quaternary International*, 476, 95-101.

635 Lartaud, F, Emmanuel, L, de Rafélis, M, Pouvreau, S, Renard, M. 2010a. Influence of food  
636 supply on the  $\delta^{13}\text{C}$  signature of mollusc shells: implications for palaeoenvironmental reconstitutions.  
637 *Geo-Marine Letters*, 30, 23–34. Doi: <https://doi.org/10.1007/s00367-009-0148-4>.

638 Lartaud, F., de Rafélis, M., Ropert, M., Emmanuel, L., Geairon, P., Renard, M., 2010b. Mn  
639 labelling of living oysters: artificial and natural cathodoluminescence analyses as a tool for age and  
640 growth rate determination of *C. gigas* (Thunberg, 1793) shells. *Aquaculture*, 300 (1), 206-217, doi  
641 10.1016/j.aquaculture.2009.12.018.

642 Lartaud, F., Emmanuel, L., de Rafélis, M., Ropert, M., Labourdette, N., Richardson, C.A.,  
643 Renard, M., 2010c. A latitudinal gradient of seasonal temperature variation recorded in oyster shells  
644 from the coastal waters of France and The Netherlands. *Facies*, 56, 13, doi 10.1007/s10347-009-0196-  
645 2.

646 Lazure, P., Desmare, S., 2012. Manche – Mer du Nord – Etat physique et chimique,  
647 caractéristiques physiques, courantologie. *Caractéristiques et Etat Ecologique*, 9 p.  
648 [https://www.ifremer.fr/sextant\\_doc/dcsmm/documents/Evaluation\\_initiale/MMN/EE/MMN\\_EE\\_06\\_C](https://www.ifremer.fr/sextant_doc/dcsmm/documents/Evaluation_initiale/MMN/EE/MMN_EE_06_C)  
649 [ourantologie.pdf](https://www.ifremer.fr/sextant_doc/dcsmm/documents/Evaluation_initiale/MMN/EE/MMN_EE_06_C).

650 Matthews, K.J., 1997. The establishment of a data base of neutron activation analyses of white  
651 marble. *Archaeometry*, 39, 321-332.

652 Michelaki, K., Hughes, M.J., Hancock, R.G.V., 2013. On establishing ceramic chemical  
653 groups: exploring the influence of data analysis methods and the role of the elements chosen in  
654 analysis. In: R.H. Tykot (ed.) Proceedings of the 38<sup>th</sup> International Symposium on Archeometry – May  
655 10<sup>th</sup> - 14<sup>th</sup> 2010, Tampa, Florida. *Open Journal of Archaeometry*, 1, e1.

656 Milano, S., Schöne, B.R., Gutiérrez-Zugasti, I., 2019. Oxygen and carbon stable isotopes of  
657 *Mytilus galloprovincialis* Lamarck, 1819 shells as environmental and provenance proxies. *The*  
658 *Holocene*. Doi: 10.1177/0959683619865595.

659 Monbet, Y., Bassoulet, P., 1989. Bilan des connaissances océanographiques en rade de Brest.  
660 *Rapport technique*, IFREMER, CEA/IPSN, 106 p.

661 Morrison, L., Bennion, M., Gill, S., Graham, C.T., 2019. Spatio-temporal trace element  
662 fingerprinting of king scallops (*Pecten maximus*) reveals harvesting period and location. *Science of the*  
663 *Total Environment*, 697, 134121.

664 Mouchi, V., de Rafélis, M., Lartaud, F., Fialin, M., Verrecchia E., 2013. Chemical labelling of  
665 oyster shells used for time-calibrated high resolution Mg/Ca ratios: a tool for past estimation of seasonal  
666 temperature variations. *Palaeogeography Palaeoclimatology Palaeoecology*, 373, pp. 66-74.

667 Mouchi, V., Briard, J., Gaillot, S., Argant, T., Forest, V., Emmanuel, L., 2018. Reconstructing  
668 environments of collection site from archaeological bivalve shells: case study from oysters (Lyon,  
669 France). *Journal of Archaeological Science: Reports*, 21, 1225-1235. doi: 10.1016/j.jasrep.2017.10.025.

670 Mouchi, V., Godbillot, C., Forest, V., Ulianov, A., Lartaud, F., de Rafélis, M., Emmanuel, L.,  
671 Verrecchia, E.P., 2020a. Rare earth elements in oyster shells: provenance discrimination and potential  
672 vital effects. *Biogeosciences*, 17, 2205–2217. doi: <https://doi.org/10.5194/bg-17-2205-2020>.

673 Mouchi, V., Emmanuel, L., Forest, V., Rivalan, A., 2020b. Geochemistry of bivalve shells as  
674 indicator of shore position of the 2<sup>nd</sup> century BC. *Open Quaternary*, 6, 4, 1-15. doi:  
675 <https://doi.org/10.5334/oq.65>.

676 Mouchi, V., Godbillot, C., Dupont, C., Vella, M.-A., Forest, V., Ulianov, A., Lartaud, F., de  
677 Rafélis, M., Emmanuel, L., Verrecchia, E.P., 2021. Data for the publication by Mouchi et al.  
678 "Provenance study of oyster shells by LA-ICP-MS" [Data set]. Zenodo.  
679 <http://doi.org/10.5281/zenodo.4681223>.

680 Mourier, J.-P., Floc'h, J.-P., Coubès, L., 1989. Notice explicative, Carte géol. France (1/50 000),  
681 feuille L'Isle-Jourdain (638). Orléans: BRGM, 73 p, Carte géologique par J.-P. Mourier et al., 1989.

682 Mrozek-Wysocka, M., 2014. 5. Ancient marbles: Provenance determination by archaeometric  
683 study. In: D. Michalska & M. Szcsepaniak (eds.) *Geoscience in Archaeometry. Methods and case*  
684 *studies*. Bogucki Wydawnictwo Naukowe, Poznań, 195 p.

685 Mureau, C., 2020. Consommation et exploitation des ressources animales dans l'est du Massif  
686 central et le Languedoc de la fin de l'Antiquité tardive au haut Moyen Âge. *Ph.D. thesis*, Université de  
687 Bourgogne-Franche-Comté, Dijon.

688 Normand, E., Champagne, A., et alii, 2019. Broue (Saint-Sornin – Charente-Maritime) : un site  
689 élitaire au coeur des marais charentais. *Rapport intermédiaire de fouille programmée triennale –*  
690 *campagne 2019*, SRA Nouvelle-Aquitaine – site de Poitiers, 236 p.

691 Orsoni, V., Souchu, P., Sauzade, D., 2001. Caractérisation de l'état d'eutrophisation des trois  
692 principaux étangs corses (Biguglia, Diana et Urbino), et proposition de renforcement de leur  
693 surveillance. Rapport final. R.INT.DEL/CO 00-02. <https://archimer.ifremer.fr/doc/00074/18534>.

694 Platel, J.-P., Moreau, P., Vouvé, J., Colmont, G.R., 1977. Notice explicative, Carte géol. France  
695 (1/50 000), feuille Pons (707). Orléans: BRGM, 43 p, Carte géologique par J.-P. Platel et al., 1977.

696 Platel, J.-P., Moreau, P., Vouvé, J., Debenath, A., Colmont, G.R., Gabet, C., 1978. Notice  
697 explicative, Carte géol. France (1/50 000), feuille St-Agnant (682). Orléans: BRGM, 52 p, Carte  
698 géologique par J.-P. Platel et al., 1978.

699 Querré, G., Cassen, S., Calligaro, T., 2015. Témoin d'échanges au Néolithique le long de la  
700 façade atlantique : la parure en variscite des tombes de l'ouest de la France. In: N., Naudinot, L.,

701 Meignen, D., Binder, G., Querré (eds.) *Les systèmes de mobilité de la Préhistoire au Moyen Age. Actes*  
702 *des 35<sup>e</sup> rencontres internationales d'archéologie et d'histoire d'Antibes*, October 14<sup>th</sup>-16<sup>th</sup> 2014, 403-  
703 418. Editions APDCA, Antibes.

704 Ricardo, F., Pimentel, T., Génio, L., Calado, R., 2017. Spatio-temporal variability of trace  
705 elements fingerprints in cockle (*Cerastoderma edule*) shells and its relevance for tracing geographic  
706 origin. *Scientific Reports*, 7, 3475. Doi: 10.1038/s41598-017-03381-w.

707 Richardson, C.A., Collis, S.A., Ekaratne, K., Dare, P., Key, D., 1993. The age determination  
708 and growth rate of the European flat oyster, *Ostrea edulis*, in British waters determined from acetate  
709 peels of umbo growth lines. *ICES Journal of Marine Science*, 50, 493–500.

710 Robin, A.-K., Mouralis, D., Akköprü, Gratuze, B., Kuzucuoğlu, C., Nomade, S., Pereira, A.,  
711 Doğu, A.F., Erturaç, K., Khalidi, L., 2016. Identification and characterization of two new obsidian sub-  
712 sources in the Nemrut volcano (Eastern Anatolia, Turkey): The Sıcaksu and Kayacık obsidian. *Journal*  
713 *of Archaeological Science: Reports*, 9, 705-717.

714 Salvi, D., Mariottini, P., 2016. Molecular taxonomy in 2D: a novel ITS2 rRNA sequence  
715 structure approach guides the description of the oysters' subfamily *Saccostreinae* and the genus  
716 *Magallana* (Bivalvia: Ostreidae). *Zoological Journal of the Linnean Society*, 179, 263-276.  
717 <https://doi.org/10.1111/zoj.12455>.

718 Schneider, M., Lepetz, S., 2007. L'exploitation, la commercialisation et la consommation des  
719 huîtres à l'époque romaine en Gaule : origine géographique et source d'approvisionnement des huîtres  
720 du vieil Evreux et de Chartres. *Publication des actes du colloque 'Les nourritures de la mer, de la criée*  
721 *à l'assiette'*. Colloque de Tatihou organisé par la SFHM du 2 au 4 octobre 2003, p11-34.

722 Shackleton, N., Renfrew, C., 1970. Neolithic trade routes re-aligned by oxygen isotope analyses.  
723 *Nature*, 228, 1062-1065.

724 Sharp, Z. 2007. Principles of stable isotope geochemistry. Upper Saddle River, NJ: Pearson  
725 Prentice Hall, 360 p.



726 Somerville, L., Light, J., Allen, M.J., 2017. Marine molluscs from archaeological contexts:  
727 how they can inform interpretations of former economies and environments. *In*: M.J. Allen (Ed.)  
728 *Molluscs in Archaeology*, 214-237.

729 Sorte, C.J.B., Etter, R.J., Spackman, R., Boyle, E.E., Hannigan, R.E., 2013. Elemental  
730 fingerprinting of mussel shells to predict population sources and redistribution potential in the Gulf of  
731 Maine. *PLoS ONE*, 8, e80868.

732 Urey, H.C., Lowenstam, H.A., Epstein, S., McKinney, C.R., 1951. Measurements of  
733 paleotemperatures and temperatures of the Upper Cretaceous of England, Denmark, and the  
734 southeastern United States. *Bulletin of the Geological Society of America*, 62, 399-416.

735 van der Maaten, L. Hinton, G., 2008. Visualizing data using t-SNE. *Journal of Machine*  
736 *Learning Research*, 9, 2579-2605.

737 Vogl, J., Paz, B., Völling, E., 2019. On the ore provenance of the Trojan silver artefacts.  
738 *Archaeological and Anthropological Sciences*, 11, 3267-3277.

739 Zhao, H., Zhang, S., 2016. Effects of sediment, seawater, and season on multi-element  
740 fingerprints of Manila clam (*Ruditapes philippinarum*) for authenticity identification. *Food Control*,  
741 66, 62-68. Doi: 10.1016/j.foodcont.2016.01.045.